ISSN 1064-2269, Journal of Communications Technology and Electronics, 2023, Vol. 68, No. 9, pp. 966–970. © Pleiades Publishing, Inc., 2023.
Russian Text © The Author(s), 2023, published in Radiotekhnika i Elektronika, 2023, Vol. 68, No. 9, pp. 879–883.

ON THE 70th ANNIVERSARY OF THE INSTITUTE OF RADIOENGINEERING AND ELECTRONICS, RUSSIAN ACADEMY OF SCIENCES

Activation of a New Landslide Process on the Bureya According to Interferometric Measurements by the PALSAR-2 Radar

L. N. Zakharova[a], *, A. I. Zakharov[a], and S. A. Nikitov[b]

[a] *Kotelnikov Institute of Radioengineering and Electronics, Fryazino Branch, Russian Academy of Sciences, Fryazino, Moscow oblast, 141190 Russia*

[b] *Kotelnikov Institute of Radioengineering and Electronics, Russian Academy of Sciences, Moscow, 125009 Russia*

**e-mail: ludmila@sunclass.ire.rssi.ru*

Received May 22, 2023; revised May 24, 2023; accepted May 25, 2023

Abstract—Based on the results of processing an interferometric pair of PALSAR-2 L-band synthetic aperture radar (SAR) images taken over the territory of the Bureya landslide in May 2019 and May 2020 from the ALOS-2 satellite, a new unstable surface region has been discovered. The average monthly rate of soil displacement was estimated to be up to 1 cm/month along the slope surface at the site of the formation of a new scarp. It is noted that the materials of interferometric processing of archival data did not previously reveal any movements of the slope surface in this place. The most probable reason for the activation of the landslide process in the new area is named: a violation of stability as a result of the descent in December 2018 of the underlying landslide body.

DOI: 10.1134/S1064226923090280

INTRODUCTION

SAR interferometry [1, 2] is a valuable informative tool for monitoring dangerous technogenic and natural phenomena since it makes it possible to detect and observe small-scale undesirable deformations of scattering covers. This technique has been used for three decades to observe glaciers [3], assess the stability of transport infrastructure due to permafrost processes [4], as well as assess surface displacements as a result of earthquakes [5], landslides [6], or subsidence associated with the extraction of minerals or the construction of the subway [7, 8]. The study of such phenomena and the history of their development is very important for safe living and the preservation of industrial and residential infrastructure in the surrounding areas.

1. CHARACTERISTICS OF THE STUDY AREA

In terms of its scale, the Bureya landslide of 2018 belongs to the category of grandiose landslides: according to model [9] and ground-based measurements [10], confirmed by the results of processing satellite images [11], the landslide is about 800 m long, 400 m wide, and the volume of the landslide bed of the Bureya River soil amounted to ~19 million m^3. The consequence of the formation of the dam was an increase in the water level in the river, which threatened to flood the settlements upstream, and also posed a threat to the Bureyskaya hydropower plant (HPP) due to a possible breakthrough of the dam in the spring. To restore the watercourse in the river through a layer of landslide rocks in the period from January 22 to February 1, 2019, the forces of the Ministry of Defense of the Russian Federation carried out a series of explosions, after which they managed to form a channel, which ensured a decrease in the water level in the river above the dam.

In a series of studies [11–15], due to the processing of archival radar images by the method of SAR interferometry, it was possible to clarify the history of development at the beginning of the 21st century, of the landslide process on the Bureya River. At the first stage of studying the landslide, data from the Sentinel-1 satellites (C-band SAR, wavelength 5.6 cm) were used. It was revealed that the soil movements of the landslide slope took place at least two years before the collapse of the slope [12]. According to the same satellite data, a conclusion was made about the stability of the landslide zone in the winter of 2019, immediately after the landslide [11]. A feature of measurements on surface areas covered with forests and shrubs in the C-band was a fairly rapid loss of coherence of backscattered signals, as a result of which reliable measurements were possible only in the cold season in short time intervals between surveys (12 days, rarely 24 days).

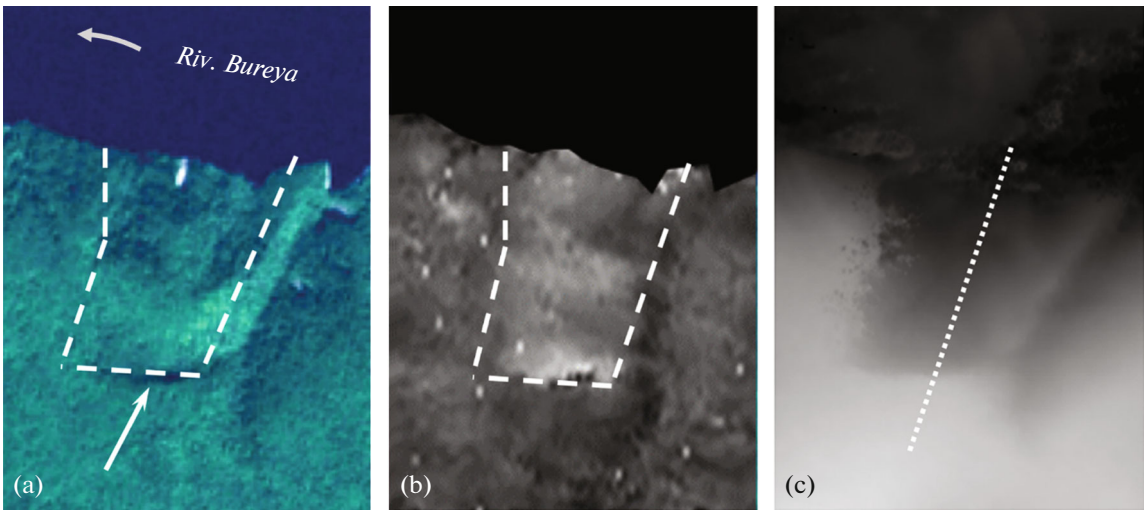

Fig. 1. Optical image (a) and interferogram (b) before the landslide (the area of the landslide is indicated by a dashed line) and a digital elevation model (c) after the landslide (the dotted line marks the position of the height profile shown below in Fig. 3); the arrow at the bottom of Fig. (a) indicates the position of the future main scarp.

Further study of the development of the dynamics of the landslide process in the period from 2006 to 2017 was performed as a result of processing the available archive images of the ALOS-1 and ALOS-2 satellites (L-band SAR, wavelength 23 cm) [13, 14]. It was found that the average speed of surface displacements increases from hardly noticeable, about 1 cm/month, at the beginning of the observation period to 6–7 cm/month at its end. In [15], based on the results of a joint analysis of radar interferometry data, highly detailed digital elevation models, and meteorological information from a ground-based weather station, possible reasons for the activation of the landslide process and the development of its dynamics from 2006 to early 2018 are outlined.

The issue of studying the stability of the surface of the landslide bowl and the surrounding area according to SAR data after the December 2018 event was given attention in several domestic studies. In [16], using the method of classical differential interferogram, it was shown that the surface of the landslide bowl after the collapse was generally stable until autumn 2019. However, due to limitations in the applicability of C-band data (high temporal decorrelation of signals in the warm season), it turned out to be impossible to observe the possible dynamics of forested surface areas adjacent to the landslide bowl. In [17], a large series of SAR images of the Sentinel-1 satellite for 2019–2020 was processed on the landslide site using the method of persistent scatterers, due to which point stably reflecting objects located on treeless areas of the surface—a landslide bowl, an earthen dam in the river bed, riverbank areas at the mouth of the Middle Sandar River were identified, and graphs of the estimated displacements of the corresponding surface parts were constructed over two years.

Judging by the interferogram constructed on the basis of the summer interferometric pair of images of 2016, the development of the landslide process up to the moment of slope collapse in December 2018 occurred within the area outlined in the optical image in Fig. 1a with the white dashed line. In this image of a forested slope, the dashed line marks the boundaries of the future landslide cirque. The fragment dimensions in Fig. 1 are 800 × 1200 m. The elevation varies from the lower (southern) edge of the fragment to the riverbank in the upper part by 400 m. The landslide main scarp will subsequently pass along a dark horizontal strip: a hollow marked with an arrow. Figure 1b shows a fragment of the interferogram constructed from the ALOS-2 data and covering a 28-day time interval in the summer of 2016 for the same territory. The phase on the river surface in the upper part of the interferogram, which is non-informative noise, is masked in black for the convenience of visual perception. Lighter tones on the interferogram correspond to moving parts of the surface of the landslide slope. According to the phase difference of the surface signals within and outside the landslide, it can be argued that in the summer of 2016 the rate of movement was up to 6 cm per month.

Figure 1c shows a fragment of a digital elevation model built taking into account changes after the landslide event according to the results of radar survey by the TanDEM-X satellite constellation in 2020. The local decrease in the relief at the location of the landslide bowl is shown in by a dark spot in Fig. 1c with almost straight edges. The boundaries of the formed landslide bowl in Fig. 1c are close to the boundaries of

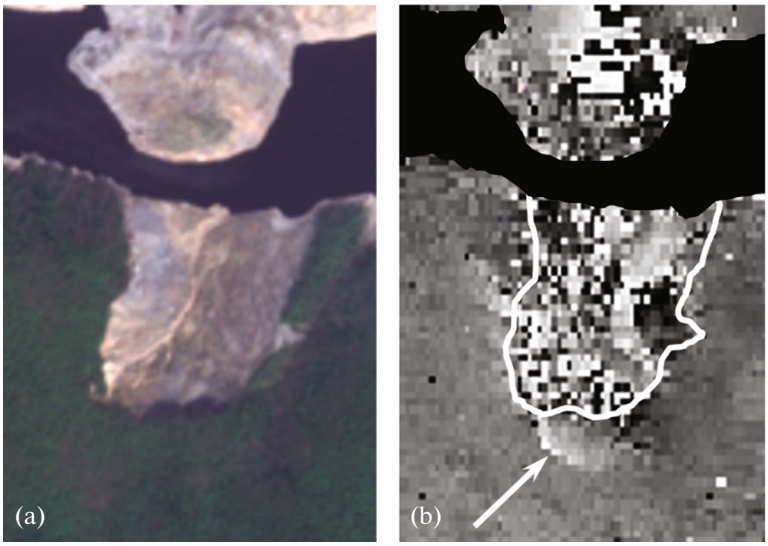

Fig. 2. Fragments of images obtained in 2019–2020 after the landslide: (a) optical Sentinel-2; (b) interferogram.

the unstable surface region revealed in the 2016 interferogram in Fig. 1b (marked with a dashed line). It should be noted that the area of surface movements in its southern part does not go beyond the landslide zone marked in Fig. 1b.

2. PROCESSING RESULTS

In this paper, an interferometric pair of images from the Japanese PALSAR-2 radar was used to identify the dynamics of the forested area near the landslide bowl taken in May 2019 and 2020. As noted in [13, 14], a feature of observations in the L-band is the increased stability of the backscattered signal, due to which, on the differential interferogram, it became possible to measure the movements of not only treeless, but also forested surface areas, which could occur during the year between surveys. New data on the dynamics of the landslide slope, obtained using the 2019–2020 interferogram, indicate that, despite the overall relative stability of the surface of the landslide bowl, a new area of instability has formed, located on the slope above the landslide main scarp.

Figure 2 shows an optical image and an interferogram characterizing the state of the landslide slope in 2019–2020. The landslide bowl in Fig. 2a is clearly visible against the background of the surrounding forested surface. An embankment that formed after the landslide in the middle of a river bed has the same sandy color as the bowl of the landslide in Fig. 2a. The free part of the riverbed (channel) runs directly at the foot of the landslide slope. The motley pattern on the interferogram within the bowl and on the embankment can be explained by repeated small collapses of the soil, due to which the coherence of signal backscatter decreases. A new detail on the interferogram in Fig. 2b, the light segment, marked with an arrow, is an activated landslide, the size of which across the slope (from west to east) is about 300 m, and along the slope (from north to south) is about 150 m. The location of the moving section directly above the main scarp is threatening to collapse. Another detail on the interferogram (Fig. 2b), related to the surface dynamics, is located inside the contour of the already descended landslide. In the western part of the bowl, due to low coherence, interferometry cannot provide information about the slips, but in the eastern part, the picture is smoother: a general light tone and a black spot in the area of the triangular ledge of the landslide contour. A sharp border between black and white in this place indicates a phase ambiguity when passing through value 2π, so that, in general, the phase values are increased relative to the values on neighboring slopes, which in the selected processing scheme indicates a shift down the slope, and the shift values are maximum in the black region and average about 1 cm per month over a 1-year interval between surveys carried out May 15, 2019 and May 13, 2020.

Figure 3 shows the height profiles along the landslide slope before and after the landslide, and also marks the position of the new moving section. The profiles were built using digital elevation models obtained using interferometric surveys by the TanDEM-X constellation in 2012 (six years before the landslide) and in 2020 (one and a half years after the landslide). The location of the profile on the height map is shown in Fig. 1c: it starts higher along the slope than the existing main scarp, runs along the entire

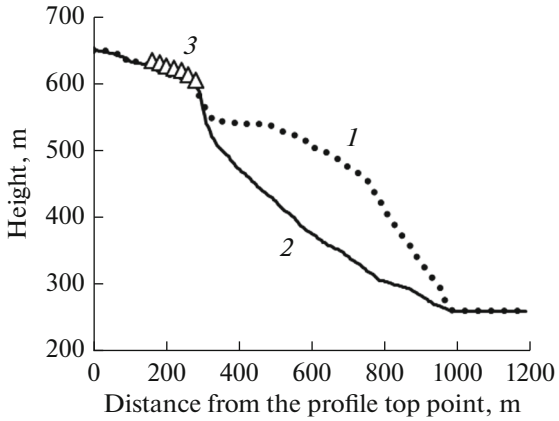

Fig. 3. Height profiles: (*1*) before the landslide, (*2*) after the landslide; (*3*) the position of the new moving section on the slope.

landslide bowl approximately in the center, and ends at the water level in the Bureya River (about 260 m above sea level).

The new movable area, marked with triangles in Fig. 3 is located on a slope at an altitude of ~400 m above the water level in the river. The average monthly displacement in the upper part of the segment in 2019 was about 1 cm (in terms of the measured 12 cm/year; it should be noted that with the change of seasons, the displacement rates may change, therefore the indicated 1 cm/month is only an average estimate). The highest displacement rate was recorded in the highest region of the site, at the site of the formation of a new main scarp (see Fig. 2b, light tone in the immediate vicinity of the white arrow pointer). The entire range of available interferometric data until December 2018 indicates that this section was stable before the landslide event. Thus, the cause of its activation seems to be the disappearance of the support in the form of landslide masses descended down the slope. It can be assumed that the activated landslide process will continue to develop further and end with a new large descent of landslide soil. Given that the width of the hole in the river at the foot of the landslide is about 150 m, there is a danger of its overlap and the emergence of a new natural hazard in the form of flooding of settlements.

CONCLUSIONS

Thanks to the use of PALSAR-2 L-band radar data, it was possible to identify a new area of movements on the bank slope of the Bureya River, which is located in the immediate vicinity of the large-scale landslide that came down in 2018 and is higher than the previously formed landslide bowl. Area dimensions are 150 × 300 m, the displacement for the period from May 2019 to May 2020 was 12 cm according to interferometric processing. Due to the destabilization of the slope, a new collapse of the rocky soil and blocking of the river channel is possible. The revealing of the activation of the landslide process is extremely important for predicting emergency events in the region, for ensuring the safe living of the population of the region, as well as for protecting industrial and residential infrastructure. This dangerous landslide zone requires the organization of urgent regular monitoring, primarily by radar surveillance equipment, including the advanced Kondor-FKA radar, which is scheduled to be launched in the near future.

ACKNOWLEDGMENTS

The authors would like to thank the Japanese Aerospace Agency JAXA for providing archival data from surveys with the PALSAR-2 radar, and also to the German Aerospace Agency DLR for providing TerraSAR-X data.

FUNDING

The study was supported by the state task of the Kotelnikov Institute of Radioengineering and Electronics, Russian Academy of Sciences, project no. 075-01133-22-00.

CONFLICT OF INTEREST

The authors declare that they have no conflicts of interest.

REFERENCES

1. P. A. Rosen, S. Hensley, I. R. Joughin, et al., Proc. IEEE **88**, 333 (2000). https://doi.org/10.1109/5.838084
2. W. Chang, C. Wang, C. Chu, and J. Kao, Proc. IEEE **100**, 2835 (2012). https://doi.org/10.1109/JPROC.2012.2194629
3. R. M. Goldstein, H. Engelhardt, and M. Frolich, Science **262** (5139), 1525 (1993). https://doi.org/10.1126/science.262.5139.1525
4. C. Wang, H. Zhang, B. Zhang, et al., in *Proc. IEEE IGARSS, Milan, Italy, July 26–31, 2015* (IEEE, New York, 2015), p. 634. https://doi.org/10.1109/IGARSS.2015.7326098
5. D. Massonnet, M. Rossi, C. Carmona, et al., Nature **364**, 138 (1993). https://doi.org/10.1038/364138a0
6. M. B. Kursah and Y. Wang, in *Proc. IEEE IGARSS, Japan, Yokohama, July 28–Aug. 2, 2019* (IEEE, New York, 2019), p. 939. https://doi.org/10.1109/IGARSS.2019.8898702
7. Z. Wang, G. Liu, T. Chen, et al., in *Proc. 2nd Int. Conf. Comp. Eng. Tech., Chengdu, China, Apr. 16–18, 2010* (IEEE, New York, 2010), Vol. 3, p. 222. https://doi.org/10.1109/ICCET.2010.5485843

8. D. Perissin, Z. Wang, and H. Lin, ISPRS J. Photogrammetry & Remote Sens. **73**, 58 (2012). https://doi.org/10.1016/j.isprsjprs.2012.07.002
9. A. V. Ostroukhov, V. I. Kim, and A. N. Makhinov, Sovr. Probl. Distants. Zondirov. Zemli iz Kosmosa **16** (1), 254 (2019). https://doi.org/10.21046/2070-7401-2019-16-1-254-258
10. O. V. Zerkal', A. N. Makhinov, A. V. Kudymov, et al., GeoRisk **13** (4), 18 (2019). https://doi.org/10.25296/1997-8669-2019-13-4-18-30
11. L. N. Zakharova, A. I. Zakharov, and L. M. Mitnik, Sovr. Probl. Distants. Zondirovaniya Zemli iz Kosmosa **16** (2), 69 (2019). https://doi.org/10.21046/2070-7401-2019-16-2-69-74
12. L. N. Zakharova and A. I. Zakharov, Sovr. Probl. Distants. Zondirovaniya Zemli iz Kosmosa **16** (2), 273 (2019). https://doi.org/10.21046/2070-7401-2019-16-2-273-277
13. V. G. Bondur, L. N. Zakharova, A. I. Zakharov, et al., Sovr. Probl. Distants. Zondirovaniya Zemli iz Kosmosa **16** (5), 113 (2019). https://doi.org/10.21046/2070-7401-2019-16-5-113-119
14. V. G. Bondur, L. N. Zakharova, A. I. Zakharov, et al., Issled. Zemli iz Kosmosa, No. 5, 3 (2019). https://doi.org/10.31857/S0205-9614201953-14
15. A. Zakharov and L. Zakharova, Remote Sens. **14** (20), Article No. 5218 (2022). https://doi.org/10.3390/rs14205218
16. V. G. Bondur, L. N. Zakharova, and A. I. Zakharov, Issled. Zemli iz Kosmosa, No. 6, 26 (2019). https://doi.org/10.31857/S0205-96142019626-35
17. V. Bondur, T. Chimitdorzhiev, A. Dmitriev, and P. Dagurov, Remote Sens. **13**, Article No. 5136 (2021). https://doi.org/10.3390/rs13245136